

DYNAMIC INVESTIGATION OF CU₅₀AT%AU (001) ALLOY NANO-OXIDATION BY *IN SITU* UHV TEM

by

Liang Wang

B.S., Tsinghua University, 2000

Submitted to the Graduate Faculty of

School of Engineering in partial fulfillment

of the requirements for the degree of

Master of Science

University of Pittsburgh

2005

UNIVERSITY OF PITTSBURGH

SCHOOL OF ENGINEERING

This thesis was presented

by

Liang Wang

It was defended on

March 21, 2005

and approved by

Dr. John A. Barnard, Professor, Department of Materials Science and Engineering

Dr. Jörg M.K. Wiezorek, Associate Professor, Department of Materials Science and Engineering

Thesis Advisor: Dr. Judith C. Yang, Associate Professor, Department of Materials Science and Engineering

DYNAMIC INVESTIGATION OF CU50AT%AU (001) ALLOY FILM NANO-OXIDATION
BY *IN SITU* UHV TEM

Liang Wang, M.S.

University of Pittsburgh, 2005

Elucidating the oxidation mechanism of alloy has significant practical and theoretical impact. The addition of alloying elements could substantially alter the oxidation behavior of the base metal. The aims of this thesis research are to model alloy oxidation by investigating Cu-Au oxidation using an *in situ* ultra-high vacuum transmission electron microscopy (UHV-TEM). Cu-Au system was chosen because 1) Au does not form stable oxide at the reaction conditions, thus only Cu is expected to oxidize; and 2) Our extensive prior experiments of Cu nano-oxidation. The main findings of the research on $\text{Cu}_{0.5}\text{Au}_{0.5}$ (001) oxidation as compared to Cu (001) are: 1) segregation of gold atoms to the surface delays adsorption of oxygen and thus delays the nucleation (longer incubation time); 2) addition of gold enhances the nucleation by reducing nucleation activation energy (fast nucleation rate); 3) Oxide island growth is initially limited by surface oxygen diffusion. As oxide grows, a gold build-up zone forms around the oxide and hinders further growth by inhibits Cu supply to the reaction front; 4) Oxide grows slower due to the presence of gold.

TABLE OF CONTENTS

PREFACE.....	x
1.0 INTRODUCTION	1
1.1 GENERAL INTRODUCTION.....	1
1.2 OXYGEN SURFACE DIFFUSION MODEL OF NANO-OXIDATION	3
1.2.1 Heteroepitaxy of Cu ₂ O on Cu and Cu _{1-x} Au _x surfaces.....	3
1.2.2 Oxide Nucleation	5
1.2.3 Oxide Growth.....	6
1.3 <i>In Situ</i> STUDY OF Cu NANO-OXIDATION.....	7
1.3.1 Temperature Effect on Oxide Morphology.....	7
1.3.2 Surface Orientation Effect	10
1.4 SURFACE STRUCTURE OF Cu _{1-x} Au _x BEFORE AND AFTER O ₂ EXPOSURE	14
2.0 PROJECT OBJECTIVES	18
3.0 EXPERIMENTAL PROCEDURES.....	19
3.1 Cu-Au FILM PREPARATION AND SAMPLE MOUNTING	19
3.2 <i>In Situ</i> UHV-TEM.....	21
3.3 ATOMIC FORCE MICROCOPY	23
3.4 NED AND STEM ANALYSIS	24
4.0 RESULTS ON NANO-OXIDATION OF Cu _{0.5} Au _{0.5} AND DISCUSSION.....	27
4.1 FILM STRUCTURE BEFORE OXIDATION.....	27
4.2 OXIDE NUCLEATION	28

4.3	MORPHOLOGY EVOLUTION	30
4.4	ENERGETICS OF NUCLEATION	36
4.5	OXIDE GROWTH KINETICS	42
4.5.1	Initial Linear Oxide Growth Kinetics	43
4.5.2	Self-limiting Growth Kinetics.....	45
5.0	CONCLUSIONS.....	54
6.0	FUTURE WORKS.....	55
	BIBLIOGRAPHY.....	58

LIST OF TABLES

Table 4.1 Comparison of the activation energies (ΔG^*) for nucleation of the oxide island and the apparent oxide growth activation energy (E_G) for oxide growth in oxidation of the Cu-Au alloys with different Au mole fraction (C_{Au}). [76]	52
--	----

LIST OF FIGURES

Figure 1.1 Heteroepitaxial growth of (a) Ge islands on Si (001) surface. [27] (b) Cu ₂ O islands grow on Cu _{0.5} Au _{0.5} (001) surface at 550 °C	4
Figure 1.2 The morphology of Cu ₂ O islands formed during <i>in situ</i> oxidation of Cu(001) at an oxygen partial pressure of 5x10 ⁻⁴ torr and oxidation temperatures of (a) 350°C, (b) 500°C, (c) 600°C, (d) 750°C and (e) 1000°C, (f) epitaxial relationship between Cu ₂ O and Cu(100). Reprint from Ref. [19].	9
Figure 1.3 Schematic diagram of the reconstructed ($\sqrt{2} \times 2\sqrt{2}$)R45° O-Cu(100) surface (a), and (2x1)O-Cu(110) surface (b) due to oxygen chemisorption. Filled circles: O atoms; open circles: top layer Cu atoms; shaded circles: second layer Cu atoms.....	11
Figure 1.4 TEM micrographs of oxide islands formed on (a) flat Cu(110) surface (650 °C); (b) thermally roughened surface (750 °C); and (c) faceted surface (800 °C) at the same oxygen pressure (5x10 ⁻⁴ torr) and oxidation time (~10 min) [7].....	12
Figure 1.5 TEM micrographs of oxide islands formed on Cu (111) surface at different temperature. (a) at 350 °C island growth with high saturation density; (b) at layer growth.800 °C [7].	13
Figure 1.6 Au-Cu phase diagram. The arrow denotes the composition and temperature range of present work. Also note that the order-disorder transition temperature for bulk Cu50at%Au is 410 °C.	15
Figure 1.7 Atom arrangement in (a) Cu _{0.5} Au _{0.5} L1 ₀ and (b) Cu _{0.75} Au _{0.25} L1 ₂ structure.	16
Figure 1.8 Calculated alloy composition for each layer at the CuAu (001) surface [20]. Note that the temperature in current work falls between 900 K and 1100 K.	17
Figure 3.1 (a) Si sample support and (b) sample cartridge. In the microscope, the sample cartridge was mounted upside down.	20
Figure 3.2 (a) The modified <i>in situ</i> UHV-TEM and (b) schematics of the main elements of the system.	23

Figure 3.3 Schematic ray diagram of parallel beam NED. A mini lens is used to focus the beam on to the front focal plane of the objective lens. The beam size is determined by the size of the condenser aperture. [61].	25
Figure 3.4 Schematic of an annular detector and EELS spectrometer in a STEM. [63].	26
Figure 4.1 (a) BF TEM image of $\text{Cu}_{0.5}\text{Au}_{0.5}$ film at 550 °C, (b) diffraction pattern at room temperature, (c) diffraction pattern at 550 °C.	28
Figure 4.2 (a) shape evolution of an oxide island at 600 °C, (b) NED shows double diffraction from film and oxide, (c) NED from only Cu_2O .	31
Figure 4.3 (a) Typical AFM image of the Cu_2O island, (b) line scan across the center and (c) off center. Both (b) and (c) show the inclination angle of the pyramid plane is around 7°.	33
Figure 4.4 Structure model of Cu_2O islands. (a) two dimensional projection view from [100] direction; (b) projective view showing the irregular-shaped octagon structure.	34
Figure 4.5 (a) typical AFM image of oxide islands after penetration, (b) height profile of one island.	35
Figure 4.6 The formation mechanism of indentation beneath the island. (a) growing island consumes Cu beneath, (b) indentation created when Cu atoms are used up, (c) after penetration, the island grows in lateral direction while the thickness remains the same.	36
Figure 4.7 Gibbs free energy change as a function of nuclei size. Cu-Au oxidation has smaller critical nuclei size and activation energy for nucleation.	40
Figure 4.8 Arrhenius plots for current research and previous works on Cu (001) [65] oxidation.	41
Figure 4.9 (a) STEM Z-contrast image and EDS elemental map for (b) oxygen and (c) gold.	43
Figure 4.10 Typical BF TEM images of $\text{Cu}_{0.5}\text{Au}_{0.5}$ oxidation at 650 °C at (a) $t = 5$ min, (b) $t = 10$ min (c) $t = 17$ min as well as (d) linear fit to average cross section area vs. t .	45
Figure 4.11 <i>In situ</i> bright field TEM image showing the growth of Cu_2O islands at 700 °C.	46
Figure 4.12 Plot of cross section area vs. reaction time for oxidation at 700 °C showing self-limited growth behavior. (a) growth of the four islands labeled in Figure 4.11, (b) normalized cross-section area vs. reaction time for the four islands. The transition from 3D growth to 2D growth is also indicated.	47
Figure 4.13 Schematic of the oxide islands and capture zone. Growing islands draw copper and oxygen only from the capture zone. $2R$ is the diameter of the capture zone and $2r$ is the diameter of the oxide.	48
Figure 4.14 Fitting of experimental data to linear growth law and self-limiting growth law.	51

Figure 6.1 *In situ* observation of the oxide island growth at 600 °C on Cu15at%Au (001). A transition from initially compact to fractal shape is revealed. 56

PREFACE

My first, and most earnest, acknowledgment must go to my advisor, Prof. Judith C. Yang for her supervision, and financial support. For the past two and half years Prof. Yang has been really supportive and considerate.

My special thanks go to the Frederick Seitz Materials Research Laboratory, the University of Illinois at Urbana-Champaign, where all the experimental work in this thesis was carried out. I would like to thank I. Petrov, R. Twesten, K. Colravy, S. MacLaren, M. Marshall, M. Williams, J.G. Wen, B.Q. Li, and T. Banks for their generous technical assistance and discussion. Also I own my appreciation to all my friends in UIUC, H. Chen, Z.B. Ge, J.W. Liu, K. Zhao, W. Zhang, J. Tao, G.Z. Zhang, and P.G. Wu for their countless help.

I would like to thank Dr. G.W. Zhou for training me on the environmental TEM. Also I would like to thank him and Dr. J.A. Eastman from Argonne National Laboratory for synthesizing $\text{Cu}_{0.62}\text{Au}_{0.38}$ thin films.

The time spent by the committee members and their suggestions to improve the thesis are all very much appreciated.

I am grateful to my colleagues and friends in the University of Pittsburgh, L. Li, F.T. Xu (and his wife P.P. Ye), J.H. Wu, X.T. Han, L. Sun (and her husband C. Fang), W. Gao, M. Kisa, and R. McAfee, for their assistance on countless occasions.

Finally, and most heartfelt, acknowledgment must go to my family. They are always there whenever I need them. This could not be done without them. They have my everlasting love.

1.0 INTRODUCTION

1.1 GENERAL INTRODUCTION

Classic investigations of the oxidation behavior of metals are mostly based on thermogravimetric analysis (TGA), which measures weight changes but not structural changes. Hence, classic models of oxidation assume uniform oxide film growth, yet it is well known that many metals form oxide islands (e.g. Ni [1, 2], Fe [3-5], Pd [6] and Ti [7]) initially that later coalesce into an oxide scale. The nucleation and growth processes of oxides (which is referred as nano-oxidation hereafter) are particularly important because they impact many diverse materials problems, from passivation properties [8, 9], gate oxides [10], and fuel cell reactions to the synthesis of self-assembled nano-oxide structure for optical [3], magnetic [4] or catalytic performance [11, 12].

Many elegant surface science studies have been performed using UHV scanning tunneling microscopy (STM) to watch the interaction of gases, including oxygen, on bare metal surfaces. [6, 13-15], but these studies only extend to a few monolayers.

Nevertheless, it has been recognized for a long time that the mechanism of initial stage oxidation, i.e. from the nucleation to the coalescence of thermodynamically stable oxides that occurs in the nanometer scale regime, plays a vital role in the oxidation behavior at later stages of various metals. [6, 11] Elucidating the oxidation mechanism in this transient stage would bridge the information gap between surface science study and traditional thermogravimetric analysis, and

thus provide understanding of metal oxidation from nucleation on the surface to the growth of the oxide scale.

By using *in situ* UHV-TEM with clean, well controlled reaction conditions and nanometer resolution, information inaccessible to both surface science study and traditional oxidation methods, can be ascertained. Previous works by Yang *et al.* [16-19] and Zhou *et al.* [7, 17, 19], using Cu as a model system, clearly demonstrated that heteroepitaxial concepts, used for film growth, also describes surprisingly well the nano-oxidation of metals where oxygen surface diffusion is the dominant mechanism of initial transport, nucleation and growth. By primarily using *in situ* UHV-TEM, Yang [16-19] and Zhou [7, 17, 19] have revealed a vast range of information regarding kinetics of oxide formation, their size and shape evolution, temperature, pressure and crystal orientation effects, as well as the environmental stability of the oxide.

However, many engineered materials are alloys; hence, it is critical to understand how the nucleation and growth processes of the oxides during oxidation of an alloy are affected by the presence of secondary elements, such as preferred nucleation sites in multiphase system, composition of the nucleus of a system with more than one active alloying elements, and the redistribution of alloy elements during oxide growth.

In this thesis, *in situ* studies of the initial oxidation behavior of copper-based alloys were carried out. Cu50at%Au ($\text{Cu}_{0.5}\text{Au}_{0.5}$ hereafter) (001) single crystal thin films were oxidized to model alloy nano-oxidation because of the in-depth understanding of Cu oxidation dynamics and also because both clean and oxygen modified surface structures of Cu-Au alloys have been extensively investigated [20-26]. Since Au is stable and miscible to Cu within the composition and temperature range which we investigated, only Cu_2O is expected to form uniformly in the Cu-Au alloy, which is similar to Cu oxidation. However, many differences exist between Cu and

Cu-Au that are pivotal to surface processes and, hence, will impact nano-oxidation dramatically. These differences include: 1) lattice constant (thus lattice mismatch and interfacial strain energy); 2) surface energy; 3) segregation of Au to the surface (driven by the lower surface energy of Au); 4) diffusion of Au and Cu during oxidation that will affect oxidation kinetics; 5) limited supply of Cu that may lead to self-limited growth of oxide; and 6) effect of Au on Cu activity.

1.2 OXYGEN SURFACE DIFFUSION MODEL OF NANO-OXIDATION

Yang *et al.* [16-19] proposed and demonstrated that heteroepitaxial concepts used to describe thin film growth, e.g. Ge on Si, can successfully describe the initial oxidation of Cu (001) where oxygen surface diffusion is the primary transport mechanism. Both nucleation of Cu₂O and oxide growth are controlled by oxygen surface diffusion.

1.2.1 Heteroepitaxy of Cu₂O on Cu and Cu_{1-x}Au_x surfaces

There are three possible heteroepitaxial growth modes, depending on the surface energy and lattice mismatch between the epilayer and the substrate, i.e. monolayer-by-monolayer growth mode (Frank-van der Merve or FM mode), 3D island growth (identified as Volmer-Weber or VW mode), and an intermediate case which was found by Stranski and Krastanov (SK mode) where 2D growth initially occurs followed by 3D island formation. The most important factor in determining growth mode is the strain. Ge/Si is one of the most extensively investigated SK heteroepitaxy system because it is one of the most promising system for self-assembly of Ge “quantum dots” for electronic and optoelectronic applications [27]. Figure 1.1 (a) shows Ge islands growing on Si (001) surface at 302 °C investigated by STM [27]. Figure 1.1 (b) is the

nano-oxidation of $\text{Cu}_{0.5}\text{Au}_{0.5}$ (001) at 550 °C with oxygen partial pressure of 5×10^{-4} torr by *in situ* TEM. In fact for all temperatures, low index Cu surfaces [7, 19, 28, 29] and compositions of $\text{Cu}_{1-x}\text{Au}_x$ (x ranges from 0 to 0.5) alloys films investigated, Cu_2O islands form on Cu and $\text{Cu}_{1-x}\text{Au}_x$ with cube-on-cube crystallographical orientation relationship. When compared with Ge/Si, they have striking similarities. First of all, in both cases islands grow epitaxially on the substrate (e.g. diffraction pattern in Figure 1.1 (b)). Secondly, the nucleation and growth of the islands are diffusion limited. Hence the same heteroepitaxial concept could also be used for describing nano-oxidation of Cu or Cu-Au alloy.

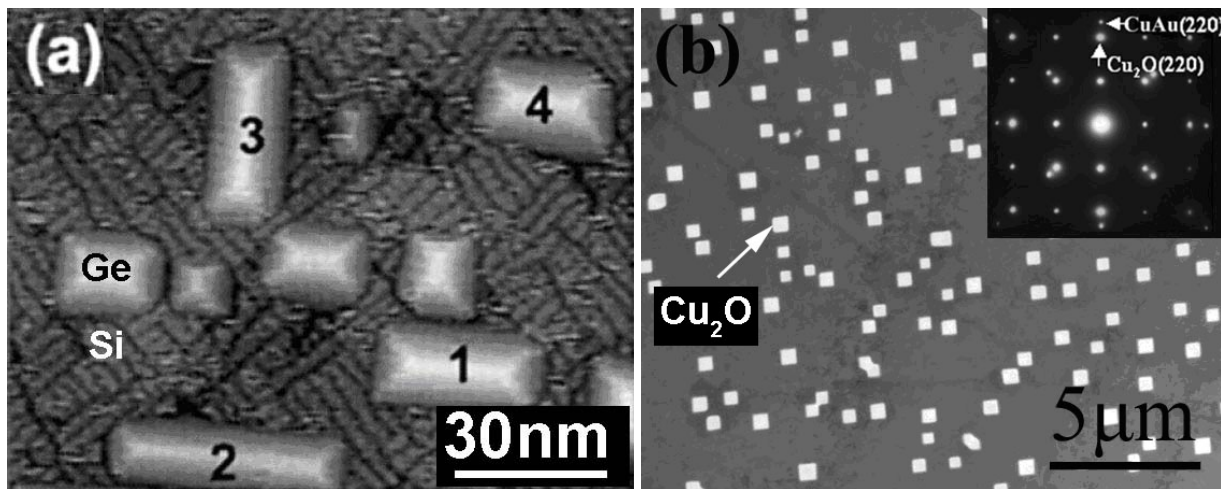


Figure 1.1 Heteroepitaxial growth of (a) Ge islands on Si (001) surface. [27] (b) Cu_2O islands grow on $\text{Cu}_{0.5}\text{Au}_{0.5}$ (001) surface at 550 °C

1.2.2 Oxide Nucleation

After admitting oxygen gas into the TEM column, the nuclei appear after an incubation time (τ_0) ranging from tens of seconds to several minutes. During this incubation time, O_2 molecules striking the film will dissociate, diffuse on the surface, and may be lost to re-evaporation, form a new nucleus, or be incorporated into an existing Cu_2O island. Regardless of the details of the intermediate steps, the density of these stable nuclei is expected to increase with time, reach a saturation density, N_s , and then decrease as the discrete nuclei grow into larger islands and coalesce. Therefore, one consequence of oxygen surface diffusion controlled nucleation is that there is a saturation island density, $1/L_d^2$, where L_d^2 is the area of the “oxygen capture zone” or “denuded zone” around each Cu_2O island. An oxygen concentration gradient exists across this zone such that oxygen that lands within this zone would diffuse to the Cu_2O islands and no other nucleation event is permitted inside this denuded zone; hence, the oxide islands act as oxygen sinks.

By assuming oxygen surface diffusion is the dominant mass transport mechanism for oxide nucleation, Yang, *et al.* demonstrated that the probability of an oxide nucleation event is proportional to the fraction of the available surface area outside these “zones of oxygen capture” and the oxide nucleus density can be determined to be [30]

$$N = \frac{1}{L_d^2} \left(1 - e^{-kL_d^2 t} \right) \quad \text{Equation 1.1}$$

where L_d^2 is the area of the zone of oxygen capture, $1/L_d^2$ is the saturation island density, L_d is much larger than the diameter of the oxide island, k is the initial nucleation rate, which depends on the probability for Cu and O to form Cu_2O at the oxidation temperature, and t is the reaction time.

The saturation island density depends on temperature and follows an Arrhenius relationship [31],

$$N_s \propto \exp(-\Delta G^* / kT) \quad \text{Equation 1.2}$$

where k is Boltzmann's constant, and T is the oxidation temperature. ΔG^* is the Gibbs free energy change to form a critical nucleus (or activation energy of nucleation) in classic nucleation theory. ΔG^* of the nucleation depends on the energies of nucleation, surface/interface energies and elastic energy changes. By Venables' nucleation rate theory [32], this ΔG^* can incorporate surface diffusion energy, nucleation energy, and desorption energy. By plotting the saturation island density at different temperatures, ΔG^* for this diffusion limited nucleation process can be determined. Also, this activation energy can also be obtained by computer simulation such as Kinetic Monte Carlo [33].

1.2.3 Oxide Growth

Orr, [34] followed by Holloway and Hudson [35], has developed an oxidation model based on the assumption that oxygen surface diffusion should play a major role in the initial growth of the metal oxide. They assumed that the 2D oxide islands grew on the metal surface and obtained a parabolic growth rate law if oxygen surface diffusion is the dominant mass transport mechanism and the reaction only occurs at the islands perimeters.

Orr's model can also be extended to 3D islands growth. Following the derivation of Orr, oxygen surface diffusion to the perimeter of an oxide island generates a growth rate [34],

$$\frac{dN(t)}{dt} = 2\pi r C_s f_s, \quad \text{Equation 1.3}$$

where $N(t)$ is the number of oxygen atoms in a Cu_2O island at time t , r is the radius of the circular profile of an island, C_s is the sticking coefficient of oxygen to a Cu_2O island, and f_s is the

diffusive flux of oxygen. For 2-D lateral growth of a disk-shaped island, with thickness a , then by solving the above differential equation, we see that the cross-sectional area increases parabolically with respect to time [34]. Following a similar analysis for 3-D growth of a spherical island, then the cross-sectional area, A , of the oxide island, is

$$A(t) = \frac{\pi\Omega C_s^2 DC_0}{D + L_d C_s} (t - t_0), \quad \text{Equation 1.4}$$

where Ω is the volume occupied by one O atom in Cu_2O , C_o is the surface concentration of oxygen far away from the Cu_2O islands, D is the surface diffusion coefficient of oxygen, L_d is the radius of the zone of oxygen capture. The power law dependence, t^2 for 2D and t for 3D, is independent of the shape of the island. On the other hand, if we know the scaling law dependence of projected areas of islands with time, it would be easy to determine whether the growth is 2D or 3D especially for TEM observation where no 3D information can be achieved.

1.3 *In Situ* STUDY OF Cu NANO-OXIDATION

1.3.1 Temperature Effect on Oxide Morphology

The temperature effect of Cu_2O islands morphologies by oxidizing Cu (100) films have been systematically studied by Yang [18], Zhou [19] and Sun [36] on the same *in situ* UHV TEM. Figure 1.2 is a reprint of the bright field (BF) TEM images from Ref. [19], which shows the morphology of Cu_2O islands formed on Cu (001) surface at different oxidation temperatures. Actually, from 200 to 350 °C [18, 19, 36], only triangular islands formed (Figure 1.2 (a)). The long edge of the triangle is indexed to be along [110] direction and the short edges are [100] and [010]. The island size increased with continued exposure to oxygen, but the island shape did not

change. At elevated temperatures, between 400 and 550 °C, the islands exhibited a shape change from triangular to square- or round-based islands (Figure 1.2 (b)). In a narrow temperature regime near 600 °C, elongated 1D Cu₂O rods formed as shown in Figure 1.2 (c). The shape formation mechanism can be explained by the energy model proposed by Tersoff and Tromp [37] where the elongated islands can efficiently release elastic strain energy stored in the oxide. Oxidation at temperatures between 650 and 800 °C resulted in the formation of dome islands, which have a distinctive cross-hatched pattern as shown in Figure 1.2 (d). At around 1000 °C, hollow terraced pyramid structure was observed, where the terrace has roughly equal step width. It is proposed that the terraced structure is formed by periodic release of compressive strain energy by slip along certain lattice plane at high temperature.

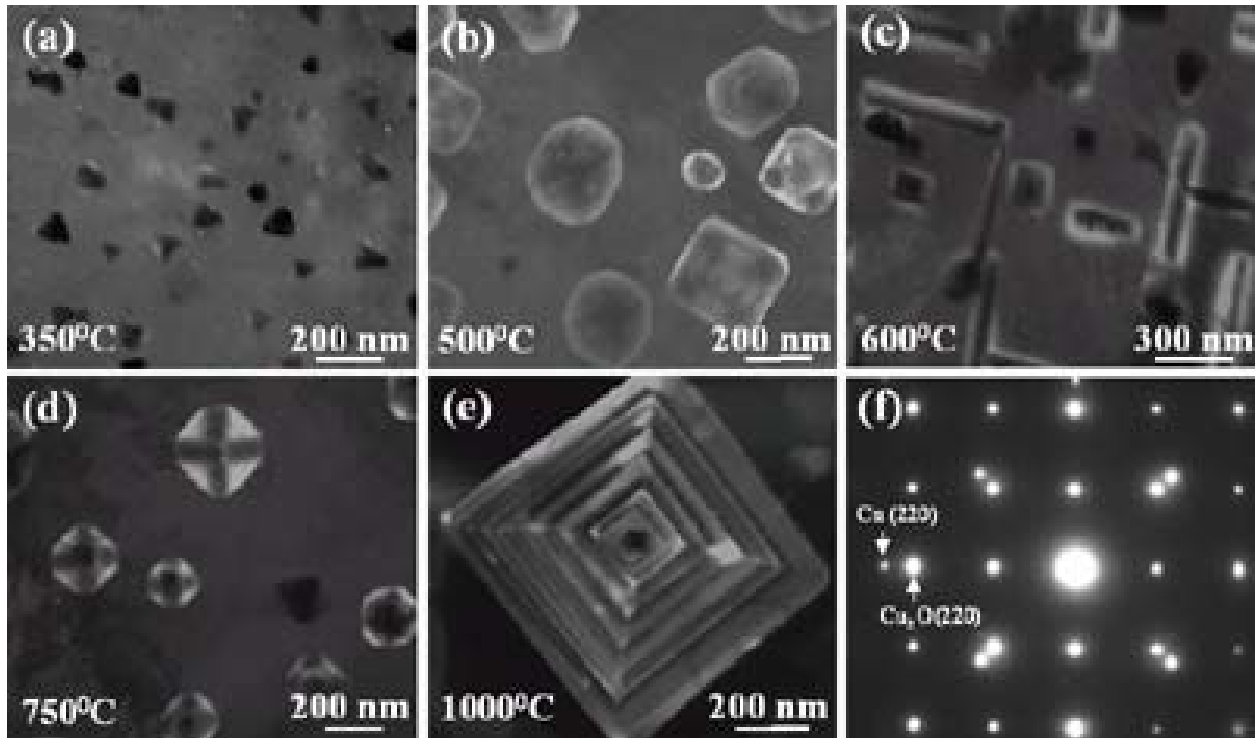


Figure 1.2 The morphology of Cu₂O islands formed during *in situ* oxidation of Cu(001) at an oxygen partial pressure of 5×10^{-4} torr and oxidation temperatures of (a) 350°C, (b) 500°C, (c) 600°C, (d) 750°C and (e) 1000°C, (f) epitaxial relationship between Cu₂O and Cu(100). Reprint from Ref. [19].

Proposed by Zhou *et al.* [19] that, energetically, balance between surface/interface energy and elastic strain energy determines the final shape of the islands. Cu₂O has a thermal expansion coefficient of $1.9 \times 10^{-6} \text{ K}^{-1}$, and Cu $17 \times 10^{-6} \text{ K}^{-1}$ [38]. With increasing temperature, the lattice mismatch becomes smaller, and the lattice mismatch induced strain becomes smaller correspondingly. This could explain the triangular shape at low temperatures, where the strain is high and so the interface area is minimized by this triangular shape. At higher temperatures, there is less lattice mismatch and therefore reducing interfacial strain with increasing

temperatures. Hence, the chosen interfaces will be along the low energy interfaces (such as the low index planes). Another effect of temperature is on the mechanical properties of the oxide and substrate. At higher temperatures, the metal substrate and oxide become significantly more ductile. The enhanced ductility at higher temperatures provides a mechanical mechanism for strain relaxation that should affect the oxide morphology development. [19]

1.3.2 Surface Orientation Effect

The initial oxidation of metal/alloy is a surface process where oxygen diffusion, oxide nucleation, and growth all occur on the alloy surface, thus the atom arrangement on the surface, i.e. surface orientation and surface composition have significant impact on the oxidation kinetics and energetics.

Gwathmey and co-workers [39-41] have demonstrated that the oxidation phenomena observed on copper vary with crystal orientation. Investigations by Benard and co-workers [42, 43] showed that the rates of oxidation were different for different crystal orientations. Zhou *et al.* [7, 28, 29] did a systematic investigation of the kinetics of the initial oxidation on Cu (100), (110) and (111) surfaces. The dependence of island density on oxidation time, saturation island density on oxidation temperature, and island growth as a function of oxidation time were all studied.

Many investigations have elegantly demonstrated that metal surfaces experience a reconstruction due to the oxygen chemisorption. Oxygen chemisorption on Cu(100) and Cu(110) results in restructuring of a surface with $(\sqrt{2} \times 2\sqrt{2})R45^\circ$ O-Cu(100) and (2×1) O-Cu(110) surface structures [44-48]. The $(\sqrt{2} \times 2\sqrt{2})R45^\circ$ O-Cu(100) has a more compact oxygen chemisorption than (2×1) O-Cu(110) surface which has a corrugated structure. Therefore, the activation barrier for surface diffusion of oxygen could be higher on the Cu(110) surface than the Cu(100). The

